# The degree of oligomerization of the H-NS nucleoid structuring protein is related to specific binding to DNA.

Cyril Badaut, Roy Williams, Véronique Arluison, Emeline Bouffartigues, Bruno Robert, Henri Buc, Sylvie Rimsky

THE JOURNAL OF BIOLOGICAL CHEMISTRY
Vol. 277, No. 44, Issue of November 1, pp. 41657–41666, 2002

*Printed in U.S.A.*

# The Degree of Oligomerization of the H-NS Nucleoid Structuring Protein Is Related to Specific Binding to DNA*

Received for publication, June 18, 2002, and in revised form, August 13, 2002
Published, JBC Papers in Press, August 27, 2002, DOI 10.1074/jbc.M206037200

**Cyril Badaut‡§¶, Roy Williams‡, Véronique Arluison‖**, Emeline Bouffartigues‡‡, Bruno Robert‖, Henri Buc‡, and Sylvie Rimsky‡ ‡‡§§**

*From the ‡URA 1773 du CNRS, Institut Pasteur, 25 Rue du Dr. Roux, 75724 Paris cedex 15, France, ‡‡Enzymologie et Cinétique Structurale, UMR 8532 Ecole Normale Supérieure de Cachan/CNRS, IGR, 39 Rue C. Desmoulins, 94805 Villejuif cedex, France, and ‖Section de Biophysique des Fonctions Membranaires, DBJC/CEA et URA CNRS 2096, Commissariat à l'Energie Atomique Saclay, 91191 Gif-sur-Yvette Cedex, France*

**At several *E. coli* promoters, initiation of transcription is repressed by a tight nucleoprotein complex formed by the assembly of the H-NS protein. In order to characterize the relationship between the structure of H-NS oligomers in solution and on relevant DNA fragments, we have compared wild-type H-NS and several transdominant H-NS mutants using gel shift assays, DNase I footprinting, analytical ultracentrifugation, and reactivity toward a cross-linking reagent. In solution, oligomerization occurs through two protein interfaces, one necessary to construct a dimeric core (and involving residues 1–64) and the other required for subsequent assembly of these dimers. We show that, as well as region 64–95, residues present in the $NH_2$-terminal coiled coil domain also participate in this second interface. Our results support the view that the same interacting interfaces are also involved on the DNA. We propose that the dimeric core recognizes specific motifs, with the second interface being critical for their correct head to tail assembly. The COOH-terminal domain of the protein contains the DNA binding motif essential for the discrimination of this specific functional assembly over competitive nonspecific H-NS polymers.**

H-NS is a DNA-binding protein involved in structurally organizing the nucleoid of prokaryotic cells. It is also involved in the regulation of many pathways, most of which are related to the response of the cell to environmental changes (1, 2). In some well characterized cases, it exerts its action at the level of transcription, either alone or in conjunction with its paralog StpA (3, 4). Both genetic and biochemical studies indicate that in this instance regulation of transcription is not mediated by a classical local interaction of H-NS with a canonical DNA sequence but rather that H-NS constitutes specific assemblies on the DNA that invade the promoter and prevent the formation of an efficient active complex between RNA polymerase and the DNA sequence (5–8). The extent of repression is also markedly sensitive to external conditions such as temperature (9), growth phase control (10, 11), or osmotic regulation (12–14). In some extreme cases, gene expression can be so severely restrained that it cannot be relieved by point mutations. In the case of the *bgl* locus in *Escherichia coli*, the ability of H-NS to polymerize along the DNA from an AT-rich crucial element appeared critical for silencing (15–18).

The formulation of a detailed mechanistic model for the action of H-NS as a repressor has been hampered by several factors. The first one is the fact that *in vitro* H-NS binds to a number of DNA sequences, affecting the efficiency of transcription of promoters located on a segment even when it does not exert any critical role on their expression *in vivo*. Using different synthetic variants of the *gal* promoter control region, containing curved or straight inserted sequences, it was possible to distinguish functional from nonfunctional assemblies. Efficient repression requires first the building up of a substructure resulting from the binding of H-NS at the curved insert (the nucleation step) and then recruitment by a cooperative process of H-NS molecules bound at other strategic sites and in particular at the Pribnow box of the *gal* control region. Subsequent to these steps, H-NS polymerizes on the DNA fragment. If a straight sequence (instead of a curved one) is inserted upstream of the promoter, full coverage may still appear on the DNA *in vitro*. However, this requires high protein concentrations. In cases where H-NS is associated with promoter regions having straight sequences, it does not generally act as a repressor *in vivo*.

At certain promoters, the control of gene expression by a distant element requires more than an initial binding at a curved sequence and propagation from this site. For instance, for the *proU* operon of *Salmonella typhimurium*, the downstream element required for action at a distance, DRE (19, 20), cannot be efficiently substituted by any other curved DNA sequence (21). A specific nucleoprotein structure, which implies also a change in the topology of the whole DNA region, must be thus constructed for efficient repression to occur (19).

H-NS exists in solution under various oligomeric forms. For some time, the nature of the lowest oligomeric state of the H-NS was a matter of debate between a model where H-NS existed as a dimer or one in which it was a trimer. Recent biophysical and structural studies characterizing the precise interface between two monomers have resolved the controversy in favor of H-NS adopting a dimer configuration as the mini-

* This work was supported by a "Program de Recherche en Biologie Fondamentale en Microbiologie et Maladies infectieuses" grant from the Ministère de l'Education Nacionale de la Recherche et de la Technologie (MNERT) and by a grant from Fondatíon pour la Recherche Médicale (FRM) supporting the creation of the "Enzymologie et cinétique structurale" group. The costs of publication of this article were defrayed in part by the payment of page charges. This article must therefore be hereby marked "*advertisement*" in accordance with 18 U.S.C. Section 1734 solely to indicate this fact.

§ Present address: URA 2185 du CNRS/Unité d'Immunologie Structurale, Institut Pasteur, 25 rue du Dr. Roux 75724, Paris cedex 15, France.

¶ Recipient of fellowships from FRM and MNERT.

** Supported by a postdoctoral fellowship from the Commissariat à l'Energie Atomique. Present address: IBPC, 13 rue P. et M. Curie, 75005 Paris, France.

§§ To whom correspondence should be addressed: IGR, 39 rue C. Desmoulins, 94805 Villejuif cedex, France. Tel.: 33-1-42-11-50-08; Fax: 33-1-42-11-52-76; E-mail: srimsky@igr.fr.

mum lowest state oligomer.[1] Earlier biophysical experiments were also satisfactorily accounted for by using a model implying the existence of two coupled equilibria of the following type,

$$4M \underset{K_1}{\longleftrightarrow} 2D \underset{K_2}{\longleftrightarrow} T$$

REACTION 1

where $M$ represents a monomer, $D$ is a dimer, and $T$ is a tetramer. The corresponding dissociation constants $K_1$ ($\sim 10^{-7}$ M) and $K_2$ ($\sim 10^{-5}$ M) are sensitive to ionic strength and to temperature (22). It is clear that a mechanistic model is needed to explain how the association interfaces involved in the oligomerization of H-NS in solution are rearranged during the formation of specific and nonspecific assemblies on a given DNA template.

To shed some light on these various issues, we have relied on the comparison between wild-type H-NS and proteins coded by dominant negative mutants of the *hns* gene, which are able to impair the normal function of the wild-type protein through the formation of wild type/mutant heterodimers or heteropolymers (23). These genetic studies as well as others led to the initial indications that H-NS consisted of two functional domains (23–26). Mutations between amino acid residues 90 and 121 reduce DNA binding activity. The latter is not affected by mutations in the amino-terminal domain between residues 12 and 65, which, however, remove repressor function. It was demonstrated that this $NH_2$-terminal part is responsible for protein-protein contacts (23, 25, 26). Three types of mutants were used in the present study: proteins modified either in the amino or the carboxyl terminus and a truncated protein containing only the first 64 amino acids of H-NS (H-NS Δ64). All of these proteins have a dominant negative effect on the wild type protein *in vivo*, implying that they are still able to interact either with wild type monomers or with the DNA. These various proteins were first compared in their ability to bind specifically to curved and to noncurved DNA fragments occurring in natural sequences where the involvement of H-NS in repression had been previously tested: the dominant negative mutants have been selected on the basis of the derepression of the *proU* operon, and the two classes of mutations display differential effects at the *proU* and *gal* modified promoters (23). We therefore selected for more specific *in vitro* assays a portion of the *proU* promoter containing the negative regulatory element, NRE. The NRE, which is the equivalent of the DRE in *S. typhimurium*, is a region of about 500 base pairs downstream of the $\sigma^{70}$-dependent promoter and overlapping the coding region for the first gene of the operon *proV*. NRE displays a region of moderate curvature centered around +196 with respect to this transcription start, and H-NS binding specificity is documented at this locus and at the upstream curved region of the promoter (20, 27–31).

The mode of association of various H-NS proteins to a *proU* linear DNA segment was analyzed by footprinting techniques. Relative binding efficiencies were compared and also related to our previous observations made on the association of WT[2] H-NS protein with *gal* modified promoters (7). Finally, the association-dissociation equilibrium of wild-type H-NS in solution was analyzed under our experimental conditions and qualitatively compared with the behavior of several altered proteins.

[1] Y. Yang, V. Bloch, E. Margeat, G. Herrada, C. Badaut, V. Arluison, B. Robert, S. Rimsky, and M. Kochoyan, submitted for publication.

[2] The abbreviations used are: WT, wild type; EDC, 1-ethyl-3-(3-dimethylaminopropyl)carbodiimide.

## EXPERIMENTAL PROCEDURES

*Purification of H-NS Proteins*—The different $His_6$-tagged H-NS proteins were expressed in *E. coli* BL21λDE3 as described by Williams *et al.* (23). Bacteria were harvested by centrifugation, resuspended in 30 ml of buffer A (40 mM phosphate buffer, pH 8.0, 0.5 M NaCl, 70 mM imidazole, and 1 mM pefabloc (Pentapharm)), and ruptured using a French press. Suspension was cleared by a 30-min centrifugation at 20,000 × *g* at 15 °C, and the supernatant was loaded on a HiTrap chelating column (Amersham Biosciences) equilibrated with a solution of A buffer supplemented with 200 mM $NiSO_4$. The column was washed with buffer A, and the H-NS proteins were eluted with a 70–500 mM gradient of imidazole in buffer A. Elution of the H-NS proteins from the column was observed at 0.15 M imidazole concentration. Prior to storage of the proteins at −20 °C, the buffer was exchanged on a PD10 column (Amersham Biosciences) for a 40 mM sodium phosphate buffer, pH 8.0, containing 0.5 M NaCl and 20% glycerol. Protein concentration was determined with a Bradford (Bio-Rad) assay using untagged wild type H-NS protein as a standard.

*Electrophoretic Mobility Shift Assays*—The 372-bp *proU* promoter DNA (extending from −68 to +303) was mixed with DNA fragments generated by digestion by *Taq*I and *Ssp*I restriction enzymes of plasmid pBR322. The final concentration of each DNA fragment was 9 nM. Samples were incubated with increasing concentrations of the different H-NS proteins for 15 min at room temperature in 40 mM Hepes, pH 8.0, 8 mM magnesium aspartate, 60 mM potassium glutamate, 0.3 mg/ml bovine serum albumin, 0.05% Nonidet P-40, and 2 mM dithiothreitol. Protein-DNA complexes were resolved on a 7.5% acrylamide/bisacrylamide (29:1) gel in TBE buffer at 20 V/cm and stained with 0.5 μg/ml ethidium bromide.

*DNase I Footprint*—The labeled 372-bp DNA *proU* fragment was generated by PCR, from the plasmid *pRWproU* (23), using the primers 5′-GCATCAATATTCATGCCA-3′ (from −69 to −53, relative to transcription start P2) and 5′-GGTGGGTTCAATCAGGC-3′ (from +287 to +302) with a combination of one unlabeled primer and the second primer end-labeled with [γ-$^{32}$]ATP (5000 Ci/mmol) by T4 polynucleotide kinase. This fragment was purified using the PCR purification kit from Roche Molecular Biochemicals. DNase I footprinting was performed using this 372-bp labeled DNA fragment following the procedure described in Ref. 7 except that the time for attack with DNase I at 25 °C was 15 s in the absence of protein and 30 s in presence of H-NS. When varying the temperature, the DNase I concentration was adjusted for each experiment in order to obtain a similar digestion profile as seen at 25 °C.

*Protein Cross-linking*—Protein cross-linking experiments were carried out using carbodiimide-mediated amide bond formation (23). The chemical cross-linker 1-ethyl-3-(3-dimethylaminopropyl)carbodiimide (EDC) reacts with the carboxyl groups of glutamate or aspartate residues to produce an unstable *O*-acetyl-isourea, which in turn forms a reactive *N*-hydroxysuccinimide ester in the presence of *N*-hydroxysuccinimide (NHS). This intermediate undergoes a nucleophilic attack by the amine group of lysine residues, leading to the formation of covalent bonds between Glu (or Asp)/Lys amino acid pairs in close proximity to each other.

Protein cross-linking reactions were performed at 100 μM protein concentration in a 40 mM HEPES buffer, pH 8, containing 8 mM magnesium aspartate, 60 mM potassium glutamate, 0.05% Nonidet P-40, and 2 mM dithiothreitol. Final concentrations of EDC and NHS in the solution were 40 and 10 mM, respectively. After incubation at room temperature for the desired amount of time, the reactions were stopped by adding 0.15 M β-mercaptoethanol and 0.1% SDS (final concentration) and heated at 95 °C for 5 min. Samples were then loaded onto an SDS-PAGE 4–20% polyacrylamide gradient gel (Bio-Rad), and the reaction products were isolated by electrophoresis, followed by Coomassie staining. Digitalization of the gel was performed on a Bio-print system (Vilbert Lourmat), and reaction products were quantified with ImageQuant software (Amersham Biosciences). All of the experimental curves have been normalized with the equation,

$$\%p_{(t)}\text{norm} = [(\%p_{(t)} - U)/R] \qquad \text{(Eq. 1)}$$

where $\%p_{(t)}$ represents the percentage of the monomer determined on the gel after time $t$, and $R$ is the yield of the reaction. $U$ represents a fraction of proteins that cannot be cross-linked to form a higher oligomeric state. The presence of this term, $U$, indicates the possible inactivation of reactants, presumably due to intramolecular reaction of those amino acids involved in the cross-linking reaction. During the cross-linking reaction, the monomer disappears with a pseudo-first

order kinetic rate, which is determined by fitting the experimental curves with the equation,

$$I_{(t)} = e^{(-k_{obs}{}^{*}t)} \quad \text{(Eq. 2)}$$

where $I_{(t)}$ is the relative intensity (in arbitrary units) of each band detected on the gel, $k_{obs}$ is the pseudo-first order rate of monomer disappearance (in $min^{-1}$) during the reaction, and $t$ is the time in minutes of the cross-linking reaction.

*Analytical Ultracentrifugation*—Equilibrium sedimentation and sedimentation velocity experiments were performed at 20 °C in a Beckman Optima XLA ultracentrifuge using an AN60-titanium Four-Holes rotor and a cell with two-channel center pieces (path length 12 mm). Prior to centrifugation, purified WT, L26P, and Δ64 proteins were dialyzed at 4 °C against 50 mM Tris-HCl, pH 6.8, containing 0.1 mM dithiothreitol and 500 mM NaCl (WT and L26P) or 200 mM NaCl (Δ64). The final concentration of H-NS proteins was 50 μM. Sedimentation velocity experiments were performed at 30,000 and 40,000 rpm for the WT and L26P proteins and 60,000 rpm for Δ64. Equilibrium sedimentation experiments were performed at 25,000 rpm. Radial scans of absorbance were taken at 280 nm for WT and L26P and 220 nm for Δ64 using dialysis buffers as reference. Sedimentation velocity data were analyzed to provide the apparent distribution of sedimentation coefficients using the program DCDT+ 1.12 (33). All measured sedimentation coefficients, $s^*$, were corrected into $s_{20,w}$ as expressed in Svedberg units using the SEDNTERP program. Equilibrium sedimentation data were analyzed to yield weight average molecular masses using the program XL-A/XL-I data analysis software 4.0 supplied by Beckman.

## RESULTS

### *Different Binding Modes of the Modified H-NS Proteins to the proU Promoter Region*

#### *Electrophoretic Mobility Shift Assays*

We used a gel retardation assay to characterize the ability of modified H-NS proteins to recognize specific DNA fragments (30, 34, 35). Digestion of a pBR322 plasmid using *Taq*I and *Ssp*I enzymes yields, in particular, a fragment carrying the *bla* promoter, which is known to contain curved sequences (36). Digested pBR was mixed in equimolar concentrations with a 372-bp DNA fragment carrying the *E. coli* control region of the *proU* promoter. The fragments were incubated with increasing concentrations of wild-type H-NS. As expected, the protein showed preferential binding for the fragment carrying the *bla* promoter, since a gel mobility shift was observed for the latter at an H-NS concentration of 0.2 μM (Fig. 1 (*I*)). The *proU* fragment was also preferentially shifted at the same protein concentration, suggesting that the wild-type H-NS protein displays approximately the same affinity for the *proU* and the *bla* promoter regions.

The same experiment was then performed with the H-NS L26P, E53G/T55P, Y97C, P116S, and I119T proteins as well as with the H-NS Δ64 truncated protein. This last polypeptide did not display any detectable affinity for the DNA fragments (not shown). With all of the other altered proteins, significant changes in the overall pattern of mobility shifts with respect to the protein concentration were observed (Fig. 1, *II–VI*). The two proteins modified in their amino-terminal domain, H-NS L26P and E53G/T55P, retained the ability to recognize specifically the same fragments as the wild-type protein (although the H-NS L26P protein had lost some affinity for the *bla* promoter region). On the other hand, the H-NS Y97C, P116S, and I119T were impaired in their ability to clearly single out the *bla* and *proU* fragments at low protein concentrations. In the presence of the modified H-NS proteins, these fragments were no longer markedly shifted with respect to the pBR322-derived ones. As a consequence, the minimum concentration needed to observe shifted fragments was higher than for WT or $NH_2$ terminus-modified proteins (1.5 μM for the H-NS Y97C as compared with 0.5 μM for the H-NS E53G/T55P; see Fig. 1, *III* and *IV*). In fact, the Y97C, P116S, and I119T proteins are modified in the carboxyl-terminal domain, which has already been suggested to be the H-NS DNA-binding domain (24). It is, however, worth noticing that these mutant proteins displayed some variations in their affinity for the fragments carrying the *bla* and *proU* promoters. The I119T mutant protein was the only one to have entirely lost its specificity for both fragments. For this mutant, the first DNA fragment of the set to be shifted by the protein was the largest one, as would be expected if this was total nonspecific binding. In contrast, the H-NS P116S, and more markedly the H-NS Y97C proteins still displayed some preferential affinity for the *proU* fragment. A gradation of effects was therefore observed in each of the two classes of dominant mutants considered. Nevertheless, the loss of recognition of specific DNA sequences was definitively localized in determinants present in the COOH-terminal domain of the protein.

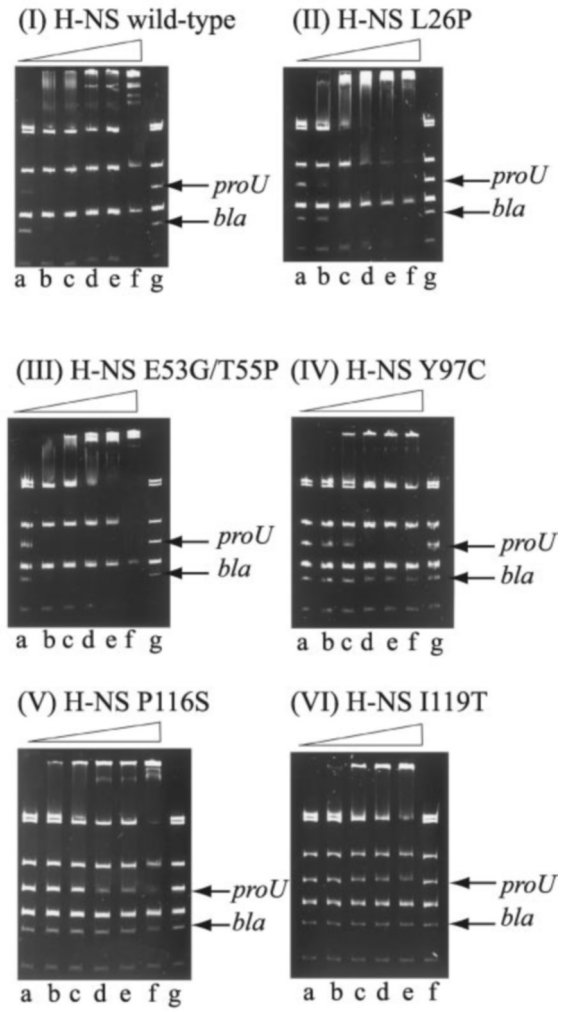


FIG. 1. **Competitive electrophoretic mobility shift assays of H-NS proteins with various DNA molecules.** Different size DNA fragments were generated by *Taq*I, *Ssp*I digestion of pBR322. A fragment (372 bp) of DNA carrying the proU promoter region was mixed with the pBR322 digest and incubated with the following. *I*, wild type H-NS (0.05, 0.2, 0.4, 0.8, 1.0, 1.2, and 0 μM in *lanes a–g*, respectively); *II*, H-NS L26P; *III*, H-NS E53G/T55P; *IV*, H-NS Y97C; *V*, H-NS P116S (0.1, 0.5, 1.0, 1.5, 2.0, 2.5, and 0 μM in *lanes a–g*, respectively); *VI*, H-NS I119T (0.5, 1.0, 1.5, 2.0, 2.5, and 0 μM in *lanes a–f*, respectively). Fragments carrying *proU* and *bla* promoter region are indicated by an *arrow*.

#### *DNase I Footprint Experiments*

*Temperature Effect*—On the *proU* DNA fragment, Lucht *et al.* (30) observed the appearance of discrete DNase I footprints for protein concentrations in the 100 nM range at room temper-

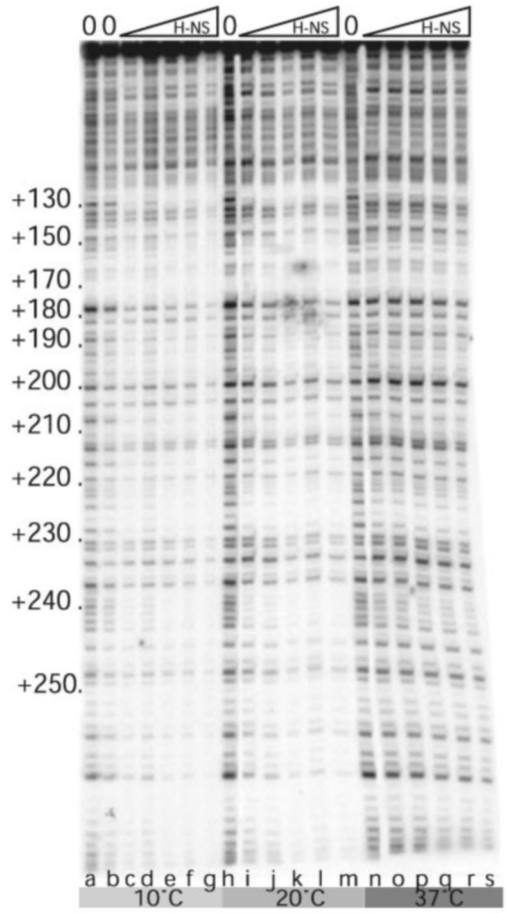


FIG. 2. **DNase I digestion pattern of the *proU* promoter coding strand in the presence of different concentrations of H-NS wild type at various temperatures.** Gel is labeled as follows: 10 °C, *lanes a–g*, 0, 0, 50, 100, 500, 1000, and 2000 nM, respectively; 20 °C, *lanes h–m*, 0, 50, 100, 500, 1000, and 2000 nM, respectively; 37 °C, *lanes n–s*, 0, 50, 100, 500, 1000, and 2000 nM, respectively.

ature. We performed similar experiments from position +130 to +280 when varying the temperature of the assay from 10 to 37 °C (Fig. 2). Binding of the wild-type H-NS protein occurred at specific sites of the *proU* fragment, at positions +130, +150/+170, +190/+200, +220/+230, and +237/+247 on the template strand (*lanes c* and *j*) at 10 and 20 °C. Increasing the H-NS concentration above 1000 nM resulted in an almost total protection of the fragment against DNase I attack (Fig. 2, *lanes g* and *m*). At 37 °C, the +130 and +220/+230 regions were still protected, but for +150/+170, +190/+200, and +237/+247, the footprints were weaker, and the extent of the protected sequence was shorter. Increasing the concentration to 1000 nM did not lead to an overall protection against DNase I attack (Fig. 2, *lanes n–s*). These results are in good agreement with the model proposed for the binding of H-NS at the *gal* modified promoters. However, temperature has a drastic effect on the binding process, inhibiting the final polymerization step and affecting the affinity of the protein for the various sites.

*Footprints Obtained with Mutant Proteins*—The protection of the DNA fragment by the mutated proteins was studied at 10 °C, the most favorable temperature for binding assays. With the H-NS E53G/T55P, the same discrete footprints were observed (Fig. 3, compare *a*, *lane b*, and *b*, *lane f*), indicating that the location of the initial binding sites was not significantly altered. However, no further modification of the pattern was observed when the protein concentration was increased to 2.5 $\mu$M (Fig. 3, compare *I* (*lanes d* and *e*) and *II* (*lanes e* and *f*)). Similar experiments performed with the H-NS L26P led to similar conclusions (Fig. 3 (*I*), *lanes g* and *h*). These experiments strongly suggest that both the E53G/T55P and the L26P proteins, altered in their $NH_2$-terminal domain, were still able to recognize nucleation sites or secondary sites on the *proU* promoter region. However, both proteins were unable to undergo the polymerization step on the DNA.

The same experiments were performed with two proteins modified in their carboxyl-terminal domain, namely the H-NS I119T and the Y97C. Both proteins, notably Y97C, previously exhibited a poor specificity of recognition of the *proU* promoter sequence among the pBR322 restriction fragments (see above). Upon DNase I attack and in the presence of increasing amounts of protein, footprints at discrete sites may still be observed, but they occurred at much higher protein concentrations than with the wild-type protein, their appearance being almost coincident with the complete protection of the fragment (Fig. 3, *I* (*lanes j–m*) and *III*).

The two proteins modified in their COOH-terminal domain were therefore still able to cover the *proU* DNA fragment, but their affinity for specific sequences was hampered. In terms of the proposed model, we suggest that the nucleation step required for the build up of a specific oligomer on the DNA is now weakened and is efficiently competed by random initiations of polymerization on the *proU* DNA fragment.

### *Oligomerization State of the Various H-NS Proteins in Solution*

#### *Analytical Ultracentrifugation*

Equilibrium sedimentation experiments were performed with the amino-terminal domain of the H-NS protein (H-NS Δ64) (Fig. 4*a*). The molecular mass determined from these experiments was 16.95 kDa. The molecular mass of each monomer, as determined by mass spectrometry, is 8240 kDa (data not shown). Under our experimental conditions, the H-NS Δ64 behaves therefore as a dimer in solution. Sedimentation velocity experiments, performed under the same experimental conditions, indeed showed the presence of a dominant species, identified here as a dimer, sedimenting at $s_{20,w}$ = 1.9 S (Fig. 4*b*).

For the wild-type H-NS, as well as for the H-NS L26P, equilibrium sedimentation experiments could not be performed, since the protein aggregated as a function of time (data not shown). Fig. 4*c* displays the distribution of sedimentation coefficients as obtained from sedimentation velocity experiments performed on the wild-type protein at a total concentration in soluble material of 50 $\mu$M. Two major species were found to be present, sedimenting at 3.9 S (76%) and at 1.8 S (24%), respectively.

When this experiment was performed with the same total concentration in the H-NS L26P, about 50% of the protein was lost due to aggregation, indicating the poor solubility of this modified H-NS under these experimental conditions. Fig. 4*d* presents a sedimentation velocity experiment performed at a total concentration in soluble material of 25 $\mu$M. As for the wild-type material, two major components were observed at 1.8 S and in the 3.8–4.5 S range. However, this time, the major component was clearly sedimenting at 1.8 S, a position matching with the slowest migrating component in the pattern observed with H-NS wild type.

At the protein concentration used in these experiments, it is clearly established that the equilibrium concentration of wild-type H-NS monomer is extremely small (22, 37). The 1.8 S component of H-NS in velocity experiments is thus at least a dimer. The presence of a species sedimenting at 1.8 S then reveals abnormal sedimentation behavior for the wild-type pro-

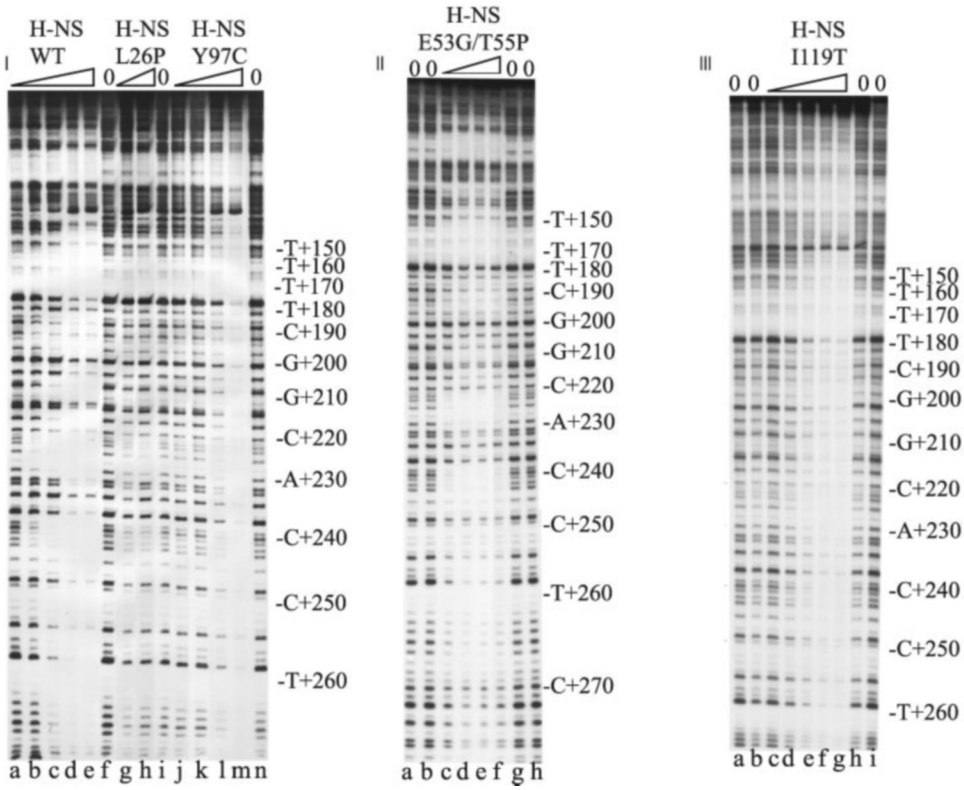


FIG. 3. **DNase I footprinting by wild type and modified H-NS on the *proU* promoter at 10 °C.** *I*, DNase I footprints on the coding strand (*lanes f*, *i*, and *n*, 0 nM H-NS). *Lanes a–e*, H-NS wild type at 0.02, 0.05, 0.15, 0.5, or 1.0 $\mu$M. *Lanes g* and *h*, 0.05 and 1 $\mu$M H-NS L26P. *Lanes j–m*, 0.05, 0.1, 0.5, or 1.0 $\mu$M H-NS Y97C. *II*, *lanes a–h*, H-NS E53G/T55P at 0, 0, 0.1, 0.5, 1.0, 2.5, 0, 0 $\mu$M, respectively. *III*, *lanes a–i*, H-NS I119T at 0, 0, 0.05, 0.1, 0.5, 1.0, 2.0, 0, and 0 $\mu$M, respectively.

tein, since this value is smaller than the one obtained for the Δ64 dimer. It must be concluded, in good agreement with recent NMR experiments (38), that the shape of the H-NS wild type is far from spherical. Indeed, the NMR signal of the whole H-NS protein was found to be strikingly similar to that of its amino-terminal domain, suggesting that the latter is moving freely in the whole protein. The aggregation state of the more slowly sedimenting component cannot be determined with accuracy, but the observation of this species clearly indicates that wild-type H-NS forms oligomeric forms higher than dimers in solution. For the H-NS L26P, the component sedimenting as a dimer represents the dominant protein form at 25 $\mu$M protein concentration.

*Protein Cross-linking*

Another way to compare the oligomerization state of the H-NS variants, and possibly to assess the association regions of the proteins that are mainly affected by the mutation, is to use a chemical cross-linking approach. A two-step chemical cross-linking reaction with the reactants EDC and NHS was performed (39). The cross-linking reaction induces formation of a peptide bond between an acidic amino acid (glutamate or aspartate) with a primary amine (lysine) when these two residues are in close contact. The efficiency of cross-linking depends mainly on the distance between the two reactive partners but also on their steric accessibility and on the ionic and hydrophilic environments of the relevant partners.

Cross-linking experiments were performed at 100 $\mu$M protein with 40 mM EDC, 10 mM NHS, as a function of reaction time. Fig. 5*A* shows experiments performed with the H-NS Δ64. As expected, a single product appeared on SDS-PAGE after cross-linking, at a position expected for a cross-linked dimer. The total yield of the reaction was 60 ± 10% after 45 min of incubation. When the wild-type H-NS was cross-linked under the same conditions, the total yield was roughly the same, but the reaction was faster. After 2 min, a cross-linked product appeared, at a position expected for a dimer (31 kDa). At later times, despite reagent inactivation higher oligomeric cross-linked products appeared as a smear in the gel. A faint band that is likely to correspond to the trimer could also be detected. We assume that this trimer results from secondary cross-links between a cross-linked dimer and one of the monomeric units of a non-cross-linked dimer. Since the interface involved in this secondary cross-link is unlikely to be the same as that comprising the dimer interface, the relative cross-linking efficiency may not be identical. Upon the appearance of the higher oligomeric forms, the percentage of cross-linked dimer remained roughly constant (Fig. 5*B*). Similar phenomena occurred with the protein modified in its carboxyl-terminal H-NS Y97C (Fig. 5*C*). By contrast, only cross-linked dimers were observed for the proteins modified in their amino-terminal domains, H-NS E53G/T55P and H-NS L26P, even after a longer cross-linking reaction time (45 min) (Fig. 5*D*). The absence of a significant amount of cross-linked oligomers larger than dimers with these proteins (as with the Δ64 polypeptide) suggests that in the two cases, protein-protein contacts are missing in one of the two interfaces, although this result as a whole may be considered as a control indicating that, under our experimental conditions, no nonspecific cross-linking occurred.

To quantitatively compare the cross-linking ability of the various proteins, we followed the kinetics of disappearance of the monomer species on the gel and monitored the overall yield of the reaction. These experiments were performed with the wild-type protein, the H-NS Δ64, and the H-NS L26P. The E53G/T55P protein exhibited a more drastic loss of cross-linking reactivity (data not shown) and was not used in the course of this experiment. The reaction conditions were first optimized by performing chemical cross-linking with various EDC and

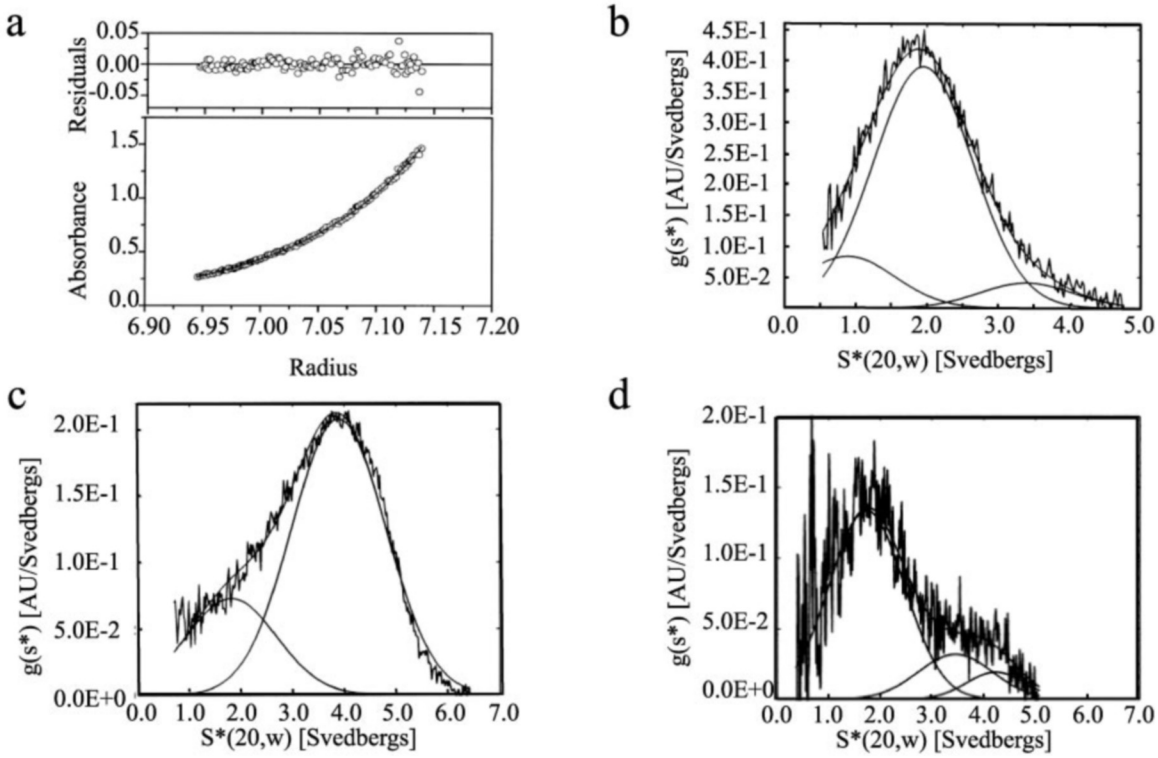


FIG. 4. *a*, absorbance *versus* radius during sedimentation equilibrium of purified Δ64 polypeptide. The *solid line* superimposed to the data corresponds to the fit used for quantifying the results. The overall weight average mass of the sample was estimated from the fit. *b*, sedimentation of $His_6$/Δ64 H-NS. The fit is shown as a *solid line* superimposed to the data. The *figure* also displays the curves obtained by deconvoluting the fitted curve into two species. *c*, sedimentation of purified $His_6$/H-NS. The fit is shown as a *solid line* superimposed to the data. *Curves*, deconvolution of the fitted curve into three species. *d*, sedimentation of purified $His_6$/H-NS L26P. The fit is shown as a *solid line* superimposed to the data.

NHS concentrations at a constant EDC/NHS ratio of 4. Increasing the concentration of EDC from 40 to 120 mM EDC resulted in a slight increase in the yield of cross-linking. The rate constant $k_{obs}$, which characterizes the exponential decay of the monomer band, depends linearly on the concentration of the chemical reactants (Fig. 6, *inset*) in this concentration range, and the reaction was pseudo-first order. At a lower concentration of 20 mM EDC, $k_{obs}$ deviated from the linear dependence for the H-NS-L26P and wild-type proteins. In conditions of pseudo-first order, the $k_{obs}$ values observed for the wild-type protein were always significantly higher than those obtained for the H-NS L26P, which were themselves higher than those measured for the H-NS Δ64. Fig. 6 displays all of the results of experiments carried out at a fixed concentration of 100 μM protein, with 40 mM EDC and 10 mM NHS as an example. The rate of decay observed for the wild-type ($k_{obs}$(WT)) is 0.14 ± 0.01 $min^{-1}$ (*i.e.* much faster than for the H-NS L26P (0.039 ± 0.001 $min^{-1}$) and for the H-NS Δ64 (0.020 ± 0.002 $min^{-1}$)).

Finally, cross-linking reactions were performed at various protein concentrations (Fig. 7), using 40 mM EDC and 10 mM NHS. For H-NS L26P and H-NS Δ64, the cross-linking reaction always led to a single species, a cross-linked dimer. In these cases, neither the yield of the cross-linked species nor the value of the rate constant, $k_{obs}$, changed significantly with protein concentration (*cf.* Fig. 7 and Table I). By contrast, $k_{obs}$ increased significantly with the concentration of the wild-type protein. The $k_{obs}$(WT) at 100 μM WT protein was 3.5-fold higher than the $k_{obs}$ of the H-NS L26P and of the H-NS Δ64. At lower wild-type protein concentration (1 μM), it became almost similar to that observed for the L26P protein ($k_{obs}$ = 0.040 $min^{-1}$).

Together with the data obtained by analytical ultracentrifugation, these results support a simple mechanism underlying the effects of the mutations on the oligomeric state of wild-type H-NS. The H-NS Δ64 domain appears to be a dimer (denoted below as core dimer) in the protein concentration range tested. The corresponding interface reacted poorly to the cross-linking reagent (low value of $k_{obs}$). The L26P protein also behaved essentially as a dimer in the cross-linking assays, although some higher oligomers were revealed by sedimentation velocity. For the wild-type protein, oligomerization states higher than the dimer have to be taken into account. Dimeric products could arise by two competing processes: cross-linking of the core dimer, occurring at the same rate as with the L26P protein (rate constant $k_1$), or cross-linking at the second interface, which probably leads to polymerization, a process which is highly concentration-dependent on the initial concentration of protein (rate constant $k_2$). The cross-linking experiments are well accounted by the simple equation,

$$k_{obs}(\mathrm{WT}) = k_1 + k_2\, p(c) \qquad \text{(Eq. 3)}$$

where ($p(c)$ represents the probability to form the second interface as a function of the total protein concentration.

## DISCUSSION

In this study, we have performed biochemical studies on wild-type H-NS and on a series of dominant negative H-NS mutants. We wanted to clarify the properties altered by these various mutations and to correlate them with previous functional studies in order to determine which protein domain is implied in a given function, and thus determine which step occurring during the formation of a nucleoprotein structure on a given DNA fragment is altered.

From the electrophoretic mobility shift assay experiments (Fig. 1), three classes of dominant negative mutants may be distinguished: (i) mutants modified in the amino-terminal domain are still able to recognize the same specific DNA targets as the wild-type protein, L26P, and E53G/T55P; (ii) mutants

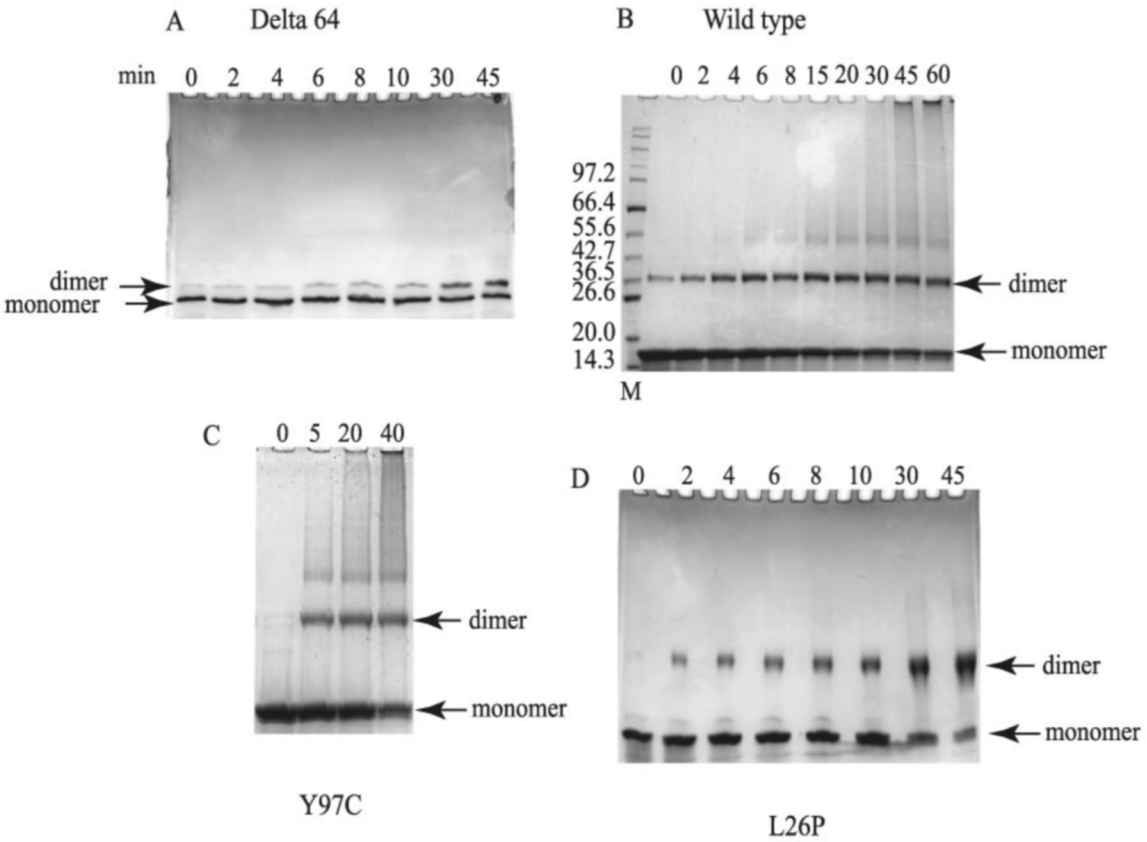


FIG. 5. **Chemically induced zero length cross-links between H-NS monomers.** Results of chemical cross-linking performed with four variants of the H-NS protein at 100 $\mu$M concentration. *A*, H-NS Δ64; *B*, H-NS WT; *C*, H-NS Y97C; *D*, H-NS L26P. Cross-linking products were isolated by SDS-PAGE and visualized by staining with Coomassie Blue. Apparent molecular mass were estimated by comparison with the relative migration of markers (*M*). Times indicated at the *top* of each *lane* represent the reaction time after the addition of the NHS/EDC before stopping the reaction by addition of stop solution as described under "Experimental Procedures."

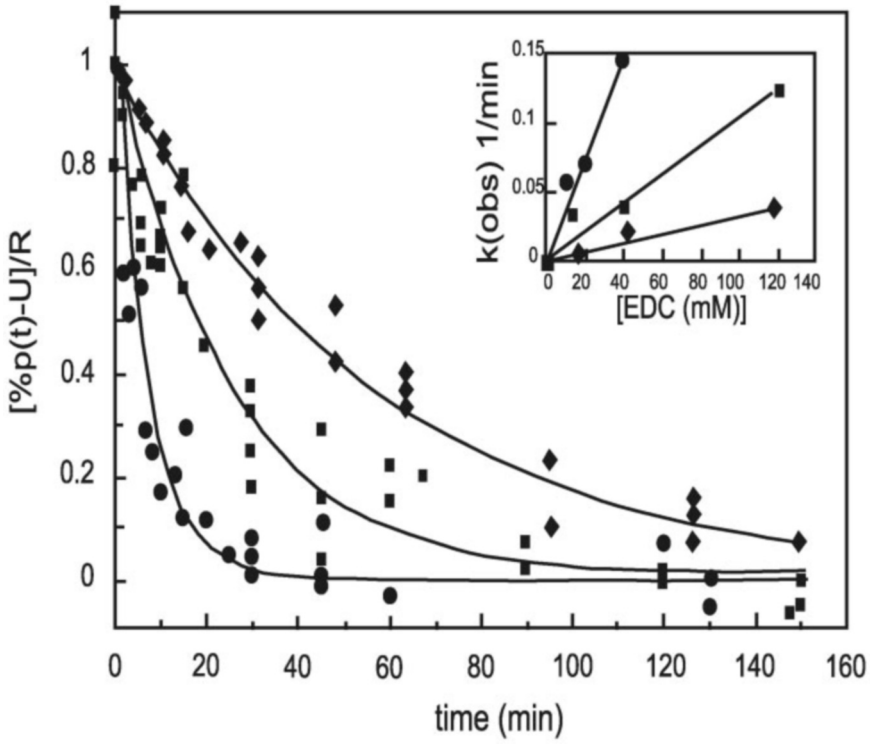


FIG. 6. **Relative intensity of Coomassie-stained bands as a function of cross-linking time.** Gels similar to those displayed in Fig. 5 were quantified, and the rates of disappearance of the monomeric form of each of the proteins (expressed as $k_{obs}$) were calculated as described under "Experimental Procedures." The *inset* shows the linear dependence of $k_{obs}$ with chemical reactant concentration for each protein. ●, H-NS WT; ■, H-NS L26P; ♦, H-NS Δ64.

modified in the carboxyl terminal domain (Y97C, P116S, and I119T) can bind to DNA but lose the ability to recognize specifically those DNA sequences preferentially bound by the WT protein, *proU* and *bla*; and (iii) one mutant (the $NH_2$-terminal Δ64 peptide) completely loses the ability to bind DNA. Different functions may therefore be clearly attributed to the two main

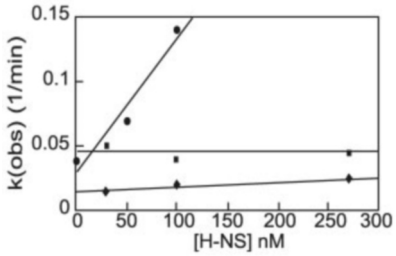


FIG. 7. **Effect of H-NS concentration on the rate of monomer disappearance following cross-linking.** Chemical cross-linking was carried out using 40 mM/10 mM EDC/NHS over a time course with varying concentrations of H-NS. The observed rate of cross-linking was calculated as described in the legend to Fig. 6 and plotted as a function of H-NS concentration. ●, H-NS WT; ■, H-NS L26P; ♦, H-NS Δ64.

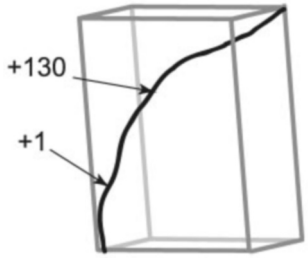


FIG. 8. **Schematic representation of the three-dimensional path traced by a 372-bp DNA fragment containing the *proU* promoter.** The DNA trajectory (based on DNA curvature model) was calculated using the program curvYX (E. Yeramiam and X. Michelet (information available upon request)) based upon the DeSantis parameters (40). The +1 denotes the start site for transcription, and +130 marks the lower limit for DNAse I footprints observed in this study.

TABLE I

*Measured rates of disappearance of H-NS monomer during EDC/NHS cross-linking as a function of total H-NS concentration*

Rates ($min^{-1}$) were calculated from curves of the type shown in Fig. 6. ND, not determined.

| H-NS concentration | WT | L26P | Δ64 |
|---|---|---|---|
| μM | | | |
| 1 | 0.039 ± 0.004 | ND | ND |
| 30 | ND | 0.050 | 0.015 |
| 50 | 0.071 ± 0.008 | ND | ND |
| 100 | 0.14 ± 0.01 | 0.039 ± 0.001 | 0.020 ± 0.002 |
| 270 | ND | 0.045 | 0.025 |

domains of the H-NS monomer. All of these results are in fair agreement with previous work reported in Ref. 25.

In *E. coli* H-NS, the basic unit (the core) is a dimer. Oligomerization of this core occurs in solution as well as when the protein is stably bound to DNA. All of the various $NH_2$-terminal domains of H-NS-like proteins examined to date are reported to be dimeric[3] with the notable exception of the Δ64 peptide from *S. typhimurium* (38). *E. coli* Δ64 H-NS analyzed here by equilibrium sedimentation behaves as a dimer. The time course of formation of cross-linked products, after reaction with EDC and N-HS, strongly suggests that this dimeric core is conserved in the integral protein. There is a marked decrease in the cross-linking efficiency after formation of the first dimeric product, a feature that is inconsistent with a rearrangement leading to a trimeric core. In fact, the overall analysis of the reactivity of the protein toward the present cross-linking reagent fully agrees with the existence of two subunit interfaces in *E. coli* H-NS, one that holds tightly the dimer and another that allows polymerization of the core. The biphasic nature of the dependence of the rate constant for monomer disappearance when the total protein concentration is increased is fairly accounted for by the lower reactivity of the polymerization interface. Indeed, the increase in the corresponding rate constant occurs in a protein concentration range where the fraction of H-NS oligomers higher than the dimer becomes significant in solution (22, 37).

Previous genetic and biochemical studies have established that the 64 $NH_2$-terminal domain of the protein is sufficient for the formation of the core (23, 26). A further extension to positions 90–95 is required for the truncated protein to display a significant amount of higher order multimers (25, 38). A naive interpretation of these results will locate the dimeric and the oligomerization interfaces in peptides 1–64 and 65–90, respectively. In agreement with this first-order approximation, we have observed that a mutant of the COOH-terminal region does not affect oligomerization in solution. Also, the removal of the residues COOH-terminal to position 64 almost completely abolishes the formation of higher oligomers, implying that the corresponding coiled coil is indeed a closed dimer. We note, however, that, in our cross-linking experiments, the Δ64 interface is less reactive than the corresponding interface in the wild-type protein (Fig. 7). This could be due to an ordering effect exerted by the 65–95 linker on the coiled-coil. Leucine 26 contributes significantly to the stability of the core interface in the coiled coil.[1] However, at a total protein concentration of 30–50 μM L26P, the destabilization exerted by this mutation is not strong enough to significantly decrease the total amount of dimer (*cf.* Fig. 7*D*). Furthermore, the biophysical properties tested (cross-linking reactivity, sedimentation constant) indicate that the L26P dimer is indeed similar to the quaternary structure adopted by the WT protein at low concentrations. Finally, the leucine to proline substitution markedly decreases the ability of this protein to form higher oligomers in solution. We conclude, therefore, that the integrity of the coiled coil domain is also required for the maintenance of a proper oligomerization interface.

It is known that efficient repression by H-NS requires not only specific protein-protein contacts but also a proper conformation of the DNA template. In this respect, the NRE region of *proU* differs from the *gal* 5A6A hybrid promoter recently analyzed for its interaction with wild-type H-NS (7). The *proU* segment under study is moderately bent (Fig. 8) but displays a series of specific sites. At low wild-type H-NS concentrations, the protein occupies the discrete sites on NRE. With increasing concentration, a general protection of the DNA against DNase I attack takes place. Bound H-NS can thus oligomerize by establishing protein-protein contacts.

As discussed in the Introduction, analysis of similar footprints on the *gal*5A6A hybrid promoter led to a mechanistic model for H-NS binding to DNA involving three steps, namely nucleation on a bent sequence; recruitment of other H-NS proteins, which result in a series of discrete footprints on the DNA fragment; and finally polymerization of H-NS along the DNA molecule. The existence of the last step essentially relies on the observation of a general protection of the DNA fragment at high protein concentration. Such a general protection may also be observed when incubating DNA with a high concentration of proteins lacking a high degree of sequence specificity. However, in the case of the H-NS protein, the total protection of DNA against DNase I attack occurs at a much lower protein concentration when a nucleation site is present in the DNA sequence (7), and repression of transcription parallels its observation. Moreover, dominant negative mutants of the H-NS protein are not able to ensure a total protection of DNA against DNase I attack (see below). It may thus be safely concluded, from footprinting experiments, that H-NS does polymerize on

[3] M. Kochoyan, personal communication.

the DNA fragment at a late stage of its binding to DNA, forming during this step a precisely defined nucleoprotein structure capable of inhibiting transcription (7). This conclusion is in good agreement with recent microscopic studies, which showed the formation of filamentous structures when visualizing H-NS·DNA complexes (41, 42). These filaments are constituted by large tracts with two regions of double-stranded DNA held close together (41). It was proposed, from their observation, that the binding of H-NS to DNA would occur through a nucleation step followed by a zipper-like propagation along the DNA (42). It is still unclear whether these images are relevant to the 372-bp fragment that was used in this work, but it is tempting to draw a parallel between the images obtained from microscopy and the footprint experiments. In this case, what we define as the polymerization step could correspond to the formation of a filament-like structure, and the propagation step in our model would represent the formation of an early nucleoprotein structure close to the curved region of DNA, necessary for the filament formation to occur. The appearance of discrete footprints (in our model of propagation following the nucleation step on the curved sequence) could correspond to the formation of a nucleoprotein complex. One way in which we are pursuing these studies is through the use of time-resolved footprinting, which will allow discrimination of specific intermediates.

Footprints obtained with the dominant negative mutants of H-NS modified in the amino-terminal domain (L26P and E53G/T55P) show that only specific sites are protected at any protein concentration. The absence of the polymerization step is thus probably due to the same alteration in protein-protein interaction as that observed in solution, the weakening of the interaction interface. The dimer formed by these mutated proteins is thus the smallest unit that can recognize and bind specifically to DNA, and this structure is probably the one involved when the core protein recognizes its specific sites on DNA prior to extensive propagation. The formation of such a fiber by the single H-NS protein requires head to tail association of the same repeating protein motif, the core dimer. The dominant negative effect of these mutants implies disruption of this type of assembly, as already postulated by Williams *et al.* (23).

The Δ64 dimer has lost its capacity to bind to DNA. However, the Δ64 protein behaves as a clear dominant negative mutant, probably because its truncated monomer can interact with a wild-type H-NS and weaken the interaction with the DNA template as well as with neighboring bound H-NS dimers, during nucleoprotein assembly.

Footprinting experiments performed with the dominant negative mutants modified in the carboxyl terminus domain show that these mutant proteins are able to induce a general protection of the DNA without prior recognition of specific sites at NRE. Cross-linking experiments performed with these mutants show that they reach the same oligomerization state as the WT protein *in vitro* (Fig. 3*D*). These mutants thus retain their full ability to form protein-protein interactions. Changes in the carboxyl-terminal domains probably induce destabilization of the hydrophobic core of the protein. It is indeed striking that most of the changes concern amino acids involved in the formation of this core, replacement residues being less hydrophobic (I119T and Y97C). This might induce an increase in the degree of freedom of the loop 90–95 to 110–115, which, as reported in Ref. 24, is important for H-NS DNA binding. It is thus unlikely that these mutants lose their ability to repress transcription, since they form different oligomers than the WT protein (43). We suggest instead an explanation in line with that invoked to explain the loss of strong repression exerted by H-NS when a straight fragment was substituted for a curved one upstream at the *gal* promoters (7). The nucleoprotein structures formed in the absence of recognition of specific sites or in the absence of a curved sequence acting as a nucleation site are more labile and therefore inefficient for the control of transcription *in vivo*.

The same set of interacting protein surfaces seems therefore to operate during the formation of oligomers in solution and as binding proceeds on a DNA template. Significant global rearrangements of the protein could, however, take place during the transfer of H-NS oligomers from solution to DNA. In solution, oligomerization rarely extends beyond the tetramer (22, 37) in the 0.2 μM to 1 mM concentration range. During their analysis of wild-type H-NS self-assembly equilibria in solution, Ceschini *et al.* have found that a temperature increase favors tetramer formation (22). On the contrary, we have found that at *proU*, polymerization is strongly hampered when the temperature was raised by 27 °C. It is not unlikely that the H-NS tetramer might undergo a significant conformational change to participate in the postulated head to tail assembly on the DNA template (*e.g.* a conversion from a closed to an open mode of polymerization). The documented flexibility of the two-domain wild-type structure could favor such a rearrangement. Furthermore, it is reported that, *in vivo* at *proU*, a temperature increase leads also to an activation of the P1 promoter (32). Therefore, changes in the strength of protein-protein contacts as well as DNA conformational changes (postulated by Falconi *et al.* (9)) could contribute to the sharp regulation exerted by temperature on prokaryotic promoters controlled by H-NS.

Finally, our experiments address the issue of specific *versus* nonspecific recognition of DNA sequences by H-NS. The binding specificity, observed by electrophoretic mobility shift assay, is correlated with the existence of discrete sites located within DNA fragments that are protected at low concentrations of wild-type proteins. How H-NS binds nonspecifically to DNA and what are the structural differences between nucleoprotein complexes built from the recognition of a specific DNA sequence and/or nonspecific sequences are questions that must be addressed in order to obtain a further understanding of H-NS function. It is important to note that the existence of these two different binding modes could help in understanding the plurality of H-NS function. Specific binding, requiring a nucleation step and polymerization of H-NS near the promoters regulated by the protein, is likely to be at the origin of the regulatory function of H-NS. Nonspecific DNA binding, due to the oligomerization of H-NS to any DNA strands, could still play a significant role in the compaction of the nucleoid exerted by H-NS.

*Acknowledgments*—We are particularly indebted to G. Batelier for help in performing analytical centrifugation experiments. We also thank J. Philo for making the computer program DCDT+ available. We thank G. Legat for technical assistance.

REFERENCES

1. Atlung, T., and Ingmer, H. (1997) *Mol. Microbiol.* **24,** 7–17
2. Hommais, F., Krin, E., Laurent-Winter, C., Soutourina, O., Malpertuy, A., Le Caer, J. P., Danchin, A., and Bertin, P. (2001) *Mol. Microbiol.* **40,** 20–36
3. Zhang, A., Rimsky, S., Reaban, M. E., Buc, H., and Belfort, M. (1996) *EMBO J.* **15,** 1340–1349
4. Free, A., Porter, M. E., Deighan, P., and Dorman, C. J. (2001) *Mol. Microbiol.* **42,** 903–917
5. Spassky, A., Rimsky, S., Garreau, H., and Buc, H. (1984) *Nucleic Acids Res.* **12,** 5321–5340
6. Schroder, O., and Wagner, R. (2000) *J. Mol. Biol.* **298,** 737–748
7. Rimsky, S., Zuber, F., Buckle, M., and Buc, H. (2001) *Mol. Microbiol.* **42,** 1311–1323
8. Caramel, A., and Schnetz, K. (2000) *Mol. Microbiol.* **36,** 85–92
9. Falconi, M., Colonna, B., Prosseda, G., Micheli, G., and Gualerzi, C. O. (1998) *EMBO J.* **17,** 7033–7043
10. Dersch, P., Schmidt, K., and Bremer, E. (1993) *Mol. Microbiol.* **8,** 875–889
11. Afflerbach, H., Schroder, O., and Wagner, R. (1998) *Mol. Microbiol.* **28,** 641–653
12. Levinthal, M., and Pownder, T. (1996) *Res. Microbiol.* **147,** 333–342
13. Barth, M., Marschall, C., Muffler, A., Fischer, D., and Hengge-Aronis, R.

(1995) *J. Bacteriol.* **177,** 3455–3464
14. Rajkumari, K., Kusano, S., Ishihama, A., Mizuno, T., and Gowrishankar, J. (1996) *J. Bacteriol.* **178,** 4176–4181
15. Schnetz, K. (1995) *EMBO J.* **14,** 2545–2550
16. Schnetz, K., and Wang, J. C. (1996) *Nucleic Acids Res.* **24,** 2422–2428
17. Mukerji, M., and Mahadevan, S. (1997) *Mol. Microbiol.* **24,** 617–627
18. Yarmolinsky, M. (2000) *Curr. Opin. Microbiol.* **3,** 138–143
19. Owen-Hughes, T., Pavitt, G. D., Santos, D. S., Sidebotham, J. M., Hulton, C. S., Hinton, J. C., and Higgins, C. F. (1992) *Cell* **71,** 255–265
20. Jordi, B. J., and Higgins, C. F. (2000) *J. Biol. Chem.* **275,** 12123–12128
21. Jordi, B., Fielder, A. E., Burns, C. M., Hinton, J. C. D., Dover, N., Ussery, D. W., and Higgins, C. F. (1997) *J. Biol. Chem.* **272,** 12083–12090
22. Ceschini, S., Lupidi, G., Coletta, M., Pon, C. L., Fioretti, E., and Angeletti, M. (2000) *J. Biol. Chem.* **275,** 729–734
23. Williams, R. M., Rimsky, S., and Buc, H. (1996) *J. Bacteriol.* **178,** 4335–4343
24. Shindo, H., Ohnuki, A., Ginba, H., Katoh, E., Ueguchi, C., Mizuno, T., and Yamazaki, T. (1999) *FEBS Lett.* **455,** 63–69
25. Ueguchi, C., Suzuki, T., Yoshida, T., Tanaka, K., and Mizuno, T. (1996) *J. Mol. Biol.* **263,** 149–162
26. Ueguchi, C., Seto, C., Suzuki, T., and Mizuno, T. (1997) *J. Mol. Biol.* **274,** 145–151
27. Gowrishankar, J. (1989) *J. Bacteriol.* **171,** 1923–1931
28. Tanaka, K., Muramatsu, S., Yamada, H., and Mizuno, T. (1991) *Mol. Gen. Genet.* **226,** 367–376
29. Tanaka, K., Ueguchi, C., and Mizuno, T. (1994) *Biosci. Biotechnol. Biochem.* **58,** 1097–1101
30. Lucht, J. M., Dersch, P., Kempf, B., and Bremer, E. (1994) *J. Biol. Chem.* **269,** 6578–6578
31. Tupper, A. E., Owen, H. Ta., Ussery, D. W., Santos, D. S., Ferguson, D. J., Sidebotham, J. M., Hinton, J. C., and Higgins, C. F. (1994) *EMBO J.* **13,** 258–268
32. Rajkumari, K., and Gowrishankar, J. (2001) *J. Bacteriol.* **183,** 6543–6550
33. Stafford, W. F. (1997) *Curr. Opin. Biotechnol.* **8,** 14–24
34. Francetic, O., Badaut, C., Rimsky, S., and Pugsley, A. P. (2000) *Mol. Microbiol.* **35,** 1506–1517
35. Timchenko, T., Bailone, A., and Devoret, R. (1996) *EMBO J.* **15,** 3986–3992
36. Hirota, Y., and Ohyama, T. (1992) *Nucleic Acids Symp. Ser.* **25,** 151–152
37. Falconi, M., Gualtieri, M. T., La Teana, A., Losso, M. A., and Pon, C. L. (1988) *Mol. Microbiol.* **2,** 323–329
38. Smyth, C. P., Lundback, T., Renzoni, D., Siligardi, G., Beavil, R., Layton, M., Sidebotham, J. M., Hinton, J. C., Driscoll, P. C., Higgins, C. F., and Ladbury, J. E. (2000) *Mol. Microbiol.* **36,** 962–972
39. Grabarek, Z., and Gergely, J. (1990) *Anal. Biochem.* **185,** 131–135
40. De Santis, P., Palleschi, A., Savino, M., and Scipioni, A. (1988) *Biophys Chem* **32,** 305–317
41. Dame, R. T., Wyman, C., and Goosen, N. (2000) *Nucleic Acids Res.* **28,** 3504–3510
42. Schneider, R., Lurz, R., Luder, G., Tolksdorf, C., Travers, A., and Muskhelishvili, G. (2001) *Nucleic Acids Res.* **29,** 5107–5114
43. Spurio, R., Falconi, M., Brandi, A., Pon, C. L., and Gualerzi, C. O. (1997) *EMBO J.* **16,** 1795–1805